Received: 1 November 2023 | Revised: 13 September 2024 | Accepted: 15 September 2024

DOI: 10.1111/ejss.13582

RESEARCH ARTICLE

European Journal of Soil Science WILEY

Remote sensing of cover crop legacies on main crop N-uptake dynamics

Nikolaos-Christos Vavlas[1] | **Thijs Seubring**[2] | **Ali Elhakeem**[1,3] | **Lammert Kooistra**[2] | **Gerlinde B. De Deyn**[1]

[1]Soil Biology Group, Wageningen University & Research, Wageningen, The Netherlands

[2]Laboratory of Geo-Information Science and Remote Sensing, Wageningen University & Research, Wageningen, The Netherlands

[3]Innovation Corridors, Agrifirm Group B.V., Apeldoorn, The Netherlands

Correspondence
Nikolaos-Christos Vavlas, Soil Biology Group, Wageningen University & Research, Droevendaalsesteeg 3, Wageningen 6708 PB, The Netherlands.
Email: nikos.vavlas@wur.nl

Funding information
Syngenta International

Abstract

Growing cover crops promotes soil health as they retain nutrients during autumn/winter and provide organic matter to the soil biota, which in turn supplies nutrients to the main crop upon mineralisation in spring. Different cover crops have varying impacts on soil biology and nutrient dynamics due to the quantity and quality of plant material returned to the soil. To understand these effects, high-resolution data on crop responses is required. In this study, remote sensing was used to provide such data. The temporal dynamics of soil nitrogen (N) availability and N uptake in barley were studied in response to different cover crop monocultures and mixtures. This was achieved using high-resolution multispectral images of the main crop acquired from an unmanned aerial vehicle. Alongside this, in-situ collected plant and soil parameters were used in this 5-year cover crop field experiment. The results showed that cover crop legacies significantly affected barley N uptake, biomass, and canopy N content. In early June, at peak canopy N, the highest values were observed in barley grown after vetch-radish or oat-radish mixtures (84 kg N/ha) and the lowest in barley grown after fallow (63 kg N) or oat (53 kg N/ha on 23rd of June). At the start of the barley growing season, soil microbial biomass was not significantly affected by the cover crop legacies. However, differential N mineralisation between cover crop legacies can be attributed to differences in microbial activity associated with cover crop quantity and quality. This research demonstrates the potential of remote sensing to monitor and understand temporal and spatial variation of crop canopy N in response to cover crop N mineralisation by the soil biota which is an important component of soil health. This approach can contribute to more efficient N use by enabling fine-tuning of the type, quantity, timing, and location of fertilisation.

KEYWORDS

barley, crop N uptake, N cycling, soil health, temporal dynamics, UAV

1 | INTRODUCTION

Optimisation of current agricultural practices to promote higher yield quantity and quality is required to meet the growing demand for food without adverse environmental impacts (Godfray et al., 2010). The key role of soils and soil biological processes is increasingly recognised as the foundation for sustainable agriculture (Fierer et al., 2021). Importantly, plant legacy or plant–soil feedback (PSF) effects on subsequent plants can be plant growth stimulating or plant growth suppressing, depending on the characteristics of the plants and their interactions with specific soil biota (Cortois et al., 2016). Therefore, trait-based crop rotations in which the impact of preceding crops on soil health is explicitly considered can improve management to optimise soil nutrient cycling and more sustainable resource use (Mariotte et al., 2018). We define soil health according to Bünemann et al. (2018) as "the continued capacity of soil to function as a vital living ecosystem that sustains plants, animals and humans", and that soil health is composed of soil physical, chemical, and biological soil properties in which nitrogen mineralisation from organic matter is a key soil biological property of high relevance to soil health in agroecosystems (Bünemann et al., 2018).

Crops are nitrogen-limited in many areas, but often N is used inefficiently and results in negative environmental effects due to overfertilisation (Erisman et al., 2013; Lassaletta et al., 2016). When crops cannot take up all the mobile forms of N supplied to soil via fertilisers, N is lost through leaching and gaseous emissions, leading to eutrophication, atmospheric pollution, groundwater contamination, and climate change (Erisman et al., 2013). To promote effective N use and counteract environmental issues, it is warranted to make better use of soil biological processes that support nutrient retention and N recycling and use less mineral N fertilisers. However, soil biological processes that underpin nutrient mineralisation from fresh and old soil organic matter (SOM) are dynamic and variable in space and time and can vary strongly within fields (Takoutsing et al., 2016). Consequently, understanding the N-cycling dynamics in agricultural systems is critical, as a good balance between soil mineral N supply and N uptake by plants is vital for sustainable crop production.

Growing cover crops can be an easily applicable management tool to generate beneficial PSF effects from cover crops to main crops. Cover crops alter soil properties during their growth as they interact with soil biota and capture nutrients and serve as fresh organic matter for soil biota after the cover crop growing season (Blanco-Canqui & Ruis, 2020; Scavo et al., 2022). However, the magnitude of PSF effects on main crops differs between cover crops and depends on plant biochemical properties and their ensuing effects on soil microbial communities (Barel et al., 2018, 2019). Important cover crop characteristics for promoting subsequent main crop growth are cover crop biomass and cover crop N concentration (Barel et al., 2018). In turn, these cover crop characteristics can be enhanced by growing mixtures of cover crop species with complementing characteristics such as N-fixation by legumes and fast N-uptake by grasses or fast-growing forbs (Ramírez-García et al., 2015; Thorup-Kristensen et al., 2003). It is well known that Brassica containing cover crops can promote cereal crops more than grass containing cover crops (Barel et al., 2018; Elhakeem et al., 2023; Holland et al., 2021). This can be explained by Brassica traits of high N uptake in autumn/winter, producing plant biomass with lower C:N and lignin compared to grasses, characteristics which result in fast N mineralisation in spring (Barel et al., 2019). Examples of brassica cover crops are mustards, oil radish, tillage radish, stubble turnip and kale.

Our rationale for testing the impact of cover crop species mixtures and those of the respective monoculture cover crops is rooted in biodiversity-ecosystem functioning research, where it has been shown that plant species mixtures composed of plant species with complementing traits are more productive (Barry et al., 2019) and potentially generate more beneficial soil legacies (Mariotte et al., 2018). In the case of cover crop mixtures composed of plant species belonging to different plant families, we combined the traits such as N fixation by the leguminous species (vetch) with the fast growth and N uptake via the fibrous root system of the grass species (bristle oat) and taproot system and fast soil cover by the brassica species (radish). From earlier cover crop experiments, we learned that increased cover crop biomass and high cover crop nitrogen concentration can promote yield of subsequent main crops, and these cover crop properties can be

Highlights

- Barley N uptake, biomass, and canopy N content ispromoted by radish-based cover crop mixtures.
- Soil microbial activity of N mineralisation is a prime soil health parameterto support sustainable cropping and is responsive to cover crop traits.
- UAV remote sensing enables high-resolution non-destructivequantification of barley canopy N content dynamics in response to cover crop legacies.

achieved by growing good combinations cover crop species (Barel et al., 2018, 2019). However, the dynamics of N uptake during main crop development in response to cover crop N mineralisation upon the activity of the soil biota remain poorly examined in the field. At the same time, we need to get better insight into these N dynamics and their temporal and spatial variability to better manage nutrient resources and counteract N losses without impairing crop development.

To avoid N leaching and promote yield quantity and quality, crop N uptake should match the availability of N in the soil from organic matter (including cover crop) mineralisation and mineral fertilisers (Elhakeem et al., 2023). Therefore, there is a need to synchronise N availability from mineralisation with N demand of the main crop during its growing season. The use of remote sensing can assist in estimating the spatial and temporal heterogeneity of N-availability in soil and N-uptake by the crops and play an informative role in fertiliser management. Understanding the dynamics of nutrient release in the soil and nutrient uptake from the plant is an integral part of proper N management, and this knowledge can be used in precision agriculture (Zhang et al., 2024). The use of remote sensing in monitoring the temporal and spatial variation of plant and soil properties is non-destructive and can enable yield predictions and plant and soil management advice at high spatial resolution (Abdulraheem et al., 2023; Cuaran & Leon, 2021; Vavlas et al., 2020).

Remote sensing–based methods to determine aboveground vegetation N are well established (Lu et al., 2021). N content has been estimated using several vegetation indices (VIs) (Näsi et al., 2018). VIs combine the surface reflectance values of at least two wavelengths to reduce background effects and strengthen the relation. Strong positive correlations are found between plant chlorophyll and N content (Ohyama, 2010). Therefore, chlorophyll-based VIs derived from remote sensing spectral data have been used to estimate variation in crop N uptake (Dong et al., 2015). According to research for assessing chlorophyll content or N uptake, red-edge chlorophyll index CI_{red} among other VI was found to have a high correlation with N content in the plant (Clevers et al., 2017; Xie et al., 2018; Yang et al., 2020). CI_{red} makes use of a positive relationship between the chlorophyll content of the canopy and the point of maximum slope between the wavelengths of 690 and 740 nm, the red edge (Jago et al., 1999). Besides VIs, other approaches, such as machine/deep learning, radiative transfer models, and hybrid techniques combining statistical and radiative transfer models, are gaining traction in the scientific community (Berger et al., 2020).

With our work, we contribute to an increased understanding of management impacts on soil health at the field scale as we quantified the dynamic parameter of N uptake in relation to cover crop legacies via their impact on soil microbial activity during the main crop season. It hence illustrates the ability of soil to function as a vital living ecosystem that sustains plants in a dynamic way at high resolution in space and time, enabled by unmanned aerial vehicle (UAV) sensor technology combined with ecological understanding of plant–soil interactions.

Effects of cover crop legacies on main crop traits can be successfully quantified using remote sensing, as has been shown for cereal and vegetable crops (Nuijten et al., 2019; van der Meij et al., 2017). However, these earlier studies focused on the final yield, N content, crop height, and volume, and did not capture the dynamics during main crop development, which is of key importance for fertilisation management. Therefore, this paper aims to examine the temporal dynamics of different cover crops on main crop development using remote sensing. We hypothesised that (i) cover crop legacies promote the N uptake of the main crop throughout the growing season and (ii) these effects can be quantified at high spatio-temporal resolution using remote sensing. We specifically compare main crop N uptake using remote sensing of the main crop grown after fallow versus after cover crops, accounting for cover crop monocultures versus mixtures. The main soil health indicator we use is the N uptake by the main crop during its development as this reflects the soil's N supply resulting from soil microbial activity by which the cover crops and inherent SOM are mineralised into plant available N. This soil health response parameter in the plants should be quantifiable non-destructively using remote sensing. We quantified additional soil health parameters: soil moisture, SOM, soil N, and soil microbial biomass to examine the potential impact of cover crop treatments on physical, chemical, and biological soil health indicators.

2 | MATERIALS AND METHODS

The soil health parameters we included are based on the review paper by Bünemann et al. (2018) comprising (i) biological indicators: soil microbial biomass and N provisioning to plants through microbial activity (quantified by plant N uptake); (ii) chemical indicators: available N, pH, and SOM; and (iii) physical indicators: soil moisture (soil texture we deemed not to be influenced by the cover crop treatments). As additional information we included soil texture parameters such as soil texture class, bulk density, and water retention curve; these were measured at the beginning of the experiment.

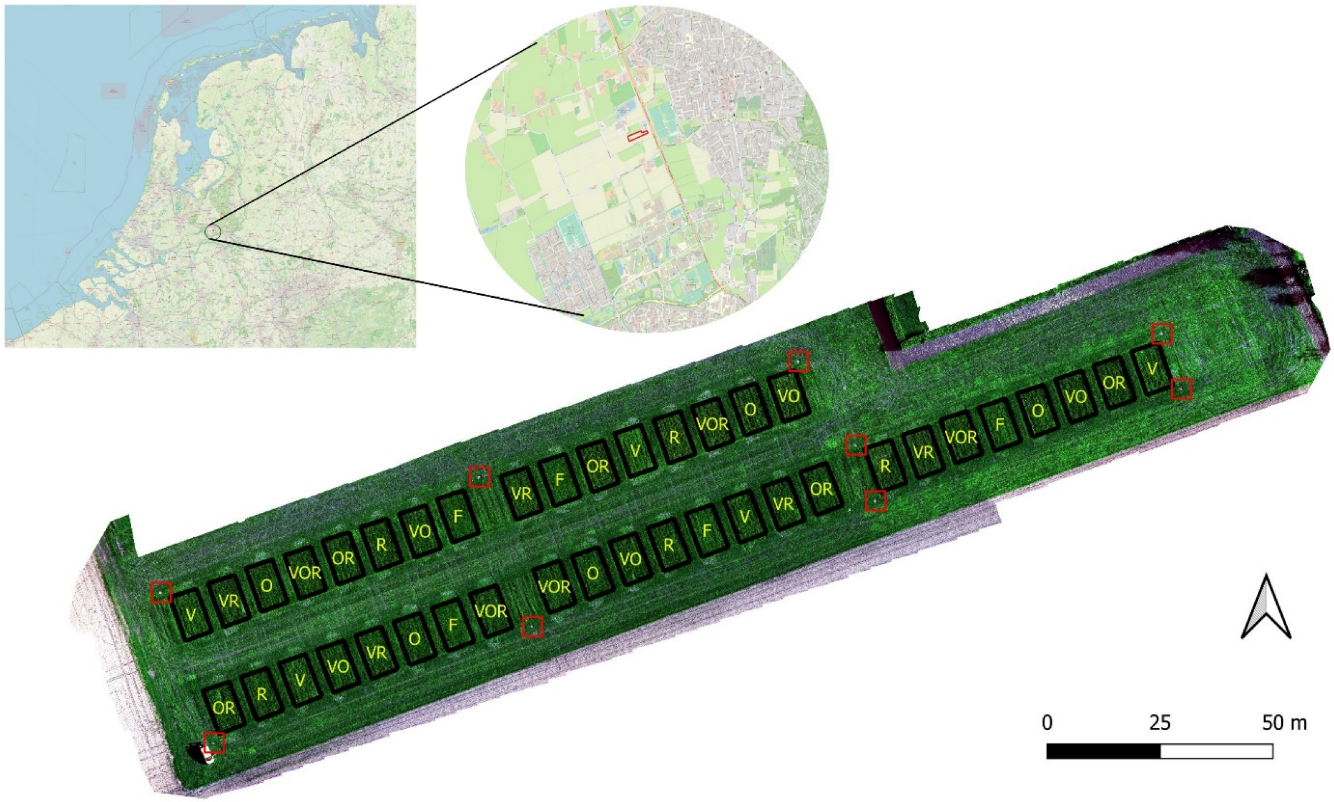

FIGURE 1 Spatial design of the field experiment with 40 plots, comprising seven different cover crop treatments and the fallow treatment replicated in five randomised blocks, as displayed in the image obtained from a drone flight (03/06/2021). The treatments comprised cover crop monocultures, and bi- and tri-species mixtures of F, fallow; O, oats; R, radish; V, vetch. Red squares display the ground control points.

2.1 | Study area

Data for the current study was collected during 2021, from the cover crop field experiment established in 2016. The site is located at the field area of Wageningen University and Research in the Netherlands (51°59′41.9″N 5°39′17.5″E). The soil is a loamy sand (86% sand) with a pH of 5.3. In this experiment, main crops are rotated with different winter cover crop treatments, with different species of main crops over the years and the same set of eight different cover crop treatments during the cover crop season (for details, see Elhakeem et al., 2023). The experimental design consists of eight cover crop treatments, each with five replicates arranged in a complete randomised block design, resulting in a total of 40 plots, each of $6 \times 10\ m^2$ (Figure 1). The cover crop treatments comprised monocultures, all pairwise mixtures and the mixture of all three species of the following cover crops: black oat (*Avena strigosa*), fodder radish (*Raphanus sativus*), and common vetch (*Vicia sativa*), and fallow plots were established as control. In August 2020, after the harvest of the main crop pea, the cover crop treatments were seeded. After the pea harvest, the aboveground biomass was removed, and the roots remained in the soil. Furthermore, after the pea crop, mineral fertiliser was not applied, whereas after a non-leguminous crop, a small amount of nitrogen may be applied to promote the fast development of non-leguminous cover crops. For the nodulation of the vetch in all years of the crop rotation, good nodulation was observed, and this did not seem to be higher after pea, and we do not think that the availability of cells of *Rhizobia* sp. was limiting for effective nodulation in our field. The seeding rate for the cover crop monocultures was 30 kg/ha for radish, 90 kg/ha for oats, and 110 kg/ha for vetch. Cover crop mixtures were created with a replacement design; to create two- and three-species mixtures, 50% and 33% of the seeding rate in monoculture were used, respectively. Data used in this study was collected from barley (*Hordeum vulgare* L.) grown in April–August 2021. On 9th March 2021, all cover crop treatments were mechanically terminated and incorporated in the soil at 15 cm depth by Unifarm employees. Two weeks later, on 26th of March, barley was sown, and on 30th April, the plots were fertilised with 81 kg N/ha (calcium ammonium nitrate: CAN 27% N) which was lower compared to the recommended 120 kg N/ha because we took the expected contribution of N mineralisation from the cover crops into account in our N budget. In our study, we observed the developmental stages of barley, starting from tillering, stem elongation, booting (Flag leaf sheath extending), heading, flowering, milk (first grains), dough (content soft but dry),

and finally, the ripening stage (hard grain). Weather, soil moisture, and temperature data were recorded throughout the growing season (Figure S1). Additional soil parameters were quantified in the experiment: SOM by loss of ignition, pH using a pH meter on soil extracted with 1 M KCl, and soil water holding capacity from the water retention curve (Tables S1 and S2).

2.2 | Soil measurements

2.2.1 | Soil moisture sensor

TMS4 sensors were used for soil moisture and temperature recordings as this sensor type is well suited for field studies (Wild et al., 2019). In each plot, we placed one TMS4 sensor and left the sensors in the field from the time of seeding till harvest. Each TMS4 logger has three temperature sensors at different heights/depths (+15, 0, −8 cm), and a soil moisture probe to measure volumetric soil moisture at approximately 0–15 cm. The loggers store data locally every 15 min for multiple years. Soil moisture was calibrated for our field site using soil samples taken on three dates and oven-dried at 105°C. Bulk density at our site was used to convert gravimetric to volumetric soil moisture.

2.2.2 | Soil mineral nitrogen

Soil samples were collected three times during the growing season: 16th of April, 27th of May, and 6th of August 2021. These dates correspond to the beginning of the crop development (3 weeks after sowing), time of stem elongation (27 days after fertilisation), and main crop harvest, respectively. Five random samples were collected per plot at each sampling time, 0–20 cm deep, using a 2-cm diameter auger. The five samples were pooled together to create one representative soil sample per plot. Pooled soil samples were dried at 40°C for 48 h then sieved over 2 mm sieve. From each sieved sample, 3 g of soil was extracted with a 0.01-M $CaCl_2$. From the extracts, soil mineral N in the form of NH_4^+ and $NO_3^- + NO_2^-$ and total extracted N (including dissolved organic N) were analysed using the segmented flow analysis system (SEAL QuAAtro segmented flow analysis system, Beunde Ronde B.V. Abcoude, The Netherlands).

To assess the in-situ mineralised N during the cropping season, we cored intact soil cylinders in the field using polypropylene cylinders (15 cm high, 6.7 cm diameter) and placed a bag of mixed bed ion-exchange resin (AmberLite MB20 H/OH, Supelco) at the bottom of each coring hole (Finney et al., 2016; Risch et al., 2019). Next, we placed the cylinder with the soil back in the coring hole on top of the resin bag to exclude root growth in the core to avoid N uptake from the soil in the cylinder (Risch et al., 2019). The cylinders were inserted into the soil on 25 May and extracted close to harvest (2 August); this period of 69 days covers the timespan from the second to the last soil sampling at plot level. The NH_4^+ and NO_3^- in the soil in the cylinders was extracted as described above, and the resin bags were extracted for NH_4^+ and NO_3^- using a 1-M KCl extraction as described in Risch et al. (2019).

2.2.3 | Soil microbial community

Microbial community biomass and composition were assessed using phospholipid lipid fatty acids (PLFA) analysis, which is well recognised for the quantifying biological indicators based on saprotrophic soil bacteria and fungi (Fierer et al., 2021; Norris et al., 2020).

For the PLFA analysis, we used the soil samples from the 16th of April campaign and extracted and quantified the PLFAs according to standard protocols, according to the Bligh and Dyer method, and based on a 2-g subsample of freeze-dried soil (Bligh & Dyer, 1959; Frostegard & Baath, 1996; Hedlund, 2002). The soil subsample was taken after sieving (2 mm) the fresh field soil right after sampling and was subsequently frozen and freeze dried. The sum of all PLFA biomarkers indicates the total microbial biomass (Zelles, 1999). We used following biomarkers markers for the bacteria (bacteria general: 15:0, Gram-positive [GP]: *i*15:0, *a*15:0, *i*16:0, *i*17:0, *a*17:0 and Gram-negative [GN]: 16:1ω9, cy17:0, 18:1ω7, cy19:0), Actinobacteria (10Me16:0, 10Me17:0, 10Me18:0), and saprotrophic fungi (18:2ω6c), based on literature (Hedlund, 2002; Heijboer et al., 2016; Martínez-García et al., 2018). The ratio of fungi to bacteria biomass (F:B) is often used to assess the effect of the agricultural practises on the microbial communities and nutrient retention (Bardgett et al., 1996). The GP to GN bacteria ratio can provide an indication of stress, with relative increase in GN bacteria indicating stress conditions (Frostegard et al., 1993; Zelles et al., 1994).

2.3 | Plant measurements

2.3.1 | Aboveground biomass

Barley was harvested on 12th of August 2021 with a combine (Haldrup). The total fresh weight of straw and grain was measured in each plot. Samples of straw and grain were collected from each plot to establish the dry matter %. All plant samples were oven-dried at 70°C for

48 h. Dried plant samples were then ball-milled to determine the concentration of C and N in straw and grain using combustion in an Element Analyser (Flash EA 1112, Thermo Scientific).

2.3.2 | SPAD sensor

To quantify the leaf nitrogen content (LNC) of the barley crop, a Minolta SPAD-502 handheld sensor was used. The sensor measures the chlorophyll content by checking the transmission of red (650 nm) and near-infrared (IR) light (940 nm) through the leaf (Markwell et al., 1995). Chlorophyll absorbs more radiation in the red wavelength compared to the near-IR wavelength. Therefore, the related chlorophyll content can be estimated by comparing light transmission at the two different wavelengths (Vos & Bom, 1993). The formula applied to transform the unitless SPAD-502 values to LNC was based on the equations derived from Boegh et al. (2013), with good fit for barley crop ($R^2 = 0.99$). This transformation is based on the following equation derived from the supplementary material (Boegh et al., 2013), filtering for barley as the crop:

$$\mathrm{LNC}\left(\mathrm{g\,N/m^2}\right) = 0.0553 * \mathrm{SPAD}. \quad (1)$$

SPAD readings from barley were measured weekly at 10 locations within each plot (Figure 2), starting from the end of April until the beginning of August (before harvest), resulting in 400 data points across the field per sampling date. SPAD readings were taken next to the midrib in the middle of the youngest fully expanded leaves; per within plot location, three measurements were performed to capture the variation per within-plot location. Therefore, per time point, a total of 30 SPAD measurements were done per plot (10 positions by three repeats), and 1200 across the field. SPAD data was collected at 13 points in time during the barley growing season (April–August 2021).

2.3.3 | UAV remote sensing

Spectral information on the crop canopy was collected by a five-band multispectral camera mounted under an UAV. The UAV was a DJI Matrice M210 V2 RTK and carried the multispectral camera MicaSense Altum to capture spectral information from the plots while flying at an altitude of 20 m. The MicaSense camera has a resolution of 2064 × 1544 pixels with ground resolution of 8.85 mm/pix. The camera collects spectral signatures for five bands simultaneously; a blue band, a green band, a red band, a red-edge band, and a near-IR band (Table 1).

The UAV data were collected throughout the growing season of barley between 8th of April and 12th of August, at 2-week intervals for a total of 13 flight days (Table S3). The Agisoft Metashape software (ver. 1.5.1, Agisoft LLC, St. Petersburg, Russia) was used to construct 3D point clouds, multispectral orthomosaics, and digital surface

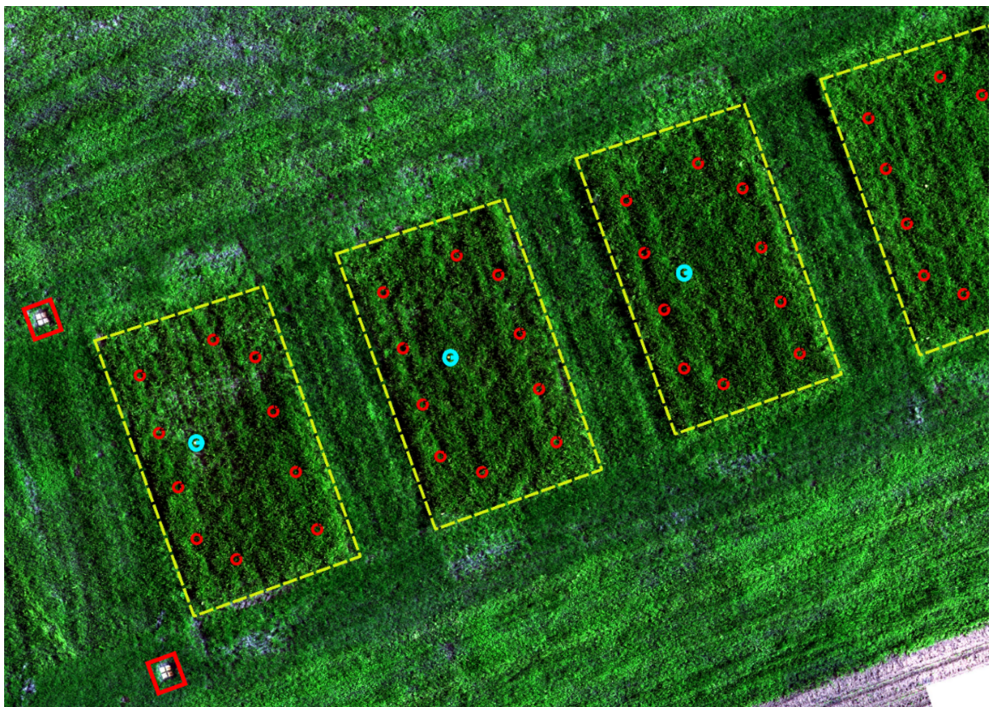

FIGURE 2 In-situ plant sampling locations (red dots), 10 per plot (yellow rectangles, plot size 6 × 10 m^2), used each sampling time. Image taken from the unmanned aerial vehicle campaign during the barley growing period (03/06/2021). The red squares indicate the ground control points and the blue circles the TMS4 soil sensors.

TABLE 1 MicaSense sensor information on the wavelengths of the five bands.

Band name	Centre wavelength (nm)	Bandwidth (nm)
Blue	475	32
Green	560	27
Red	668	14
Red edge	717	12
Near IR	842	57

Abbreviation: IR, infrared.

models. This software uses structure from motion and multiview stereo to combine the acquired images and the eight ground control points (Figure 1) into an orthomosaic (Figure 1). After georeferencing, the images were processed in QGIS and cropped to the individual plots. This created 40 individual plots per flight date and reduced the UAV images to the areas relevant to this research. The vegetation samples were taken at about 1 m distance from the edges, so that the crop was not disturbed and 0.9 m from all four edges of the plots were removed for each plot image across the growing season. This procedure aimed to reduce potential interference by other plants that grew around and in the border regions of the plots, yet to keep all the pixels that directly surrounded the barley sampling positions (more than 12 pixels in radius).

2.4 | Data processing and statistics

To assess N content in barley, VIs were calculated based on the spectral data, and subsequently related to the in-situ collected data. Soil background reflectance in an image influences the relation between VIs and vegetation properties like chlorophyll. Therefore, the first step was removing the soil pixels within the plots. Normalised difference vegetation index (NDVI) has been used to separate soil and vegetation-covered pixels within each plot and is calculated with the following formula:

$$\mathrm{NDVI} = \frac{\mathrm{NIR} - \mathrm{Red}}{\mathrm{NIR} + \mathrm{Red}}. \quad (2)$$

All pixels with a NDVI value below 0.30 were considered soil covered and removed by assigning "NoData" to them, effectively discarding those pixels from the images. This threshold showed a clear border between relevant plant values and soil background, especially during the initial period of development when the plants do not cover the entire plot, but also for later dates when the plant in senescence also results in lower plant coverage and increased influence of soil background.

The retrieval of the green leaf area index (GLAI) in plants by remote imaging is based on the $\mathrm{CI_{red}}$ VI calculation used in other studies (Kira et al., 2016; Nguy-Robertson et al., 2014).

$$\mathrm{CI_{red-edge}} = \left(\frac{\mathrm{NIR}}{\mathrm{Red_{edge}}}\right) - 1. \quad (3)$$

GLAI is needed to upscale from leaf to canopy level per plot. GLAI was calculated using the $\mathrm{CI_{red\text{-}edge}}$ (Nguy-Robertson et al., 2014). Nguy-Robertson et al. investigate the potential of determining optimal spectral bands for a universal algorithm to estimate GLAI using different crops and testing multiple spectral indices. Second-order polynomial fitting between the value of $\mathrm{CI_{red}}$ and GLAI provides the calibration of the images to display the GLAI across the plots and the equation is inverted to calculate GLAI:

$$\mathrm{CI_{red-edge}} = -0.078 * \mathrm{GLAI}^2 + 1.4 * \mathrm{GLAI} - 0.18. \quad (4)$$

The inversion is used to calculate the GLAI. The calculation of the canopy N content (CNC) combines the results of the two previous equations (Equations 3 and 4) as an indicator for the total amount of N in the plant. Initially, the CNC is calculated at the pixel level; next, the values are averaged at the plot level for each flight date to create a time-series of CNC for each treatment. Equation 5 presents the calculation of the CNC (kg N/ha):

$$\mathrm{CNC} = \mathrm{GLAI} * \mathrm{LNC}. \quad (5)$$

Cover crop legacy effects on main crop characteristics (yield, dry weight, total N and C) were examined using linear mixed effects models with the function lme from the package nlme (Pinheiro et al., 2019), including block as a random factor. Normality of the model residuals was assessed using the Shapiro test (Shapiro & Wilk, 1965), and Levene's test was used for the homogeneity of model residual variances (Levene, 1960). If the test displayed a violation of normality, then power transformation was used for that characteristic. ANOVA was used for the determination of treatment significance. The post hoc analysis aims to calculate the pairwise comparison with treatments (significance level: $a = 0.05$) using the function emmeans (Lenth et al., 2019) CLD (compact letter display of pairwise comparisons) from package multcomp (Hothorn et al., 2008).

3 | RESULTS

3.1 | Cover crop legacy effects on the main crop

The barley biomass was significantly affected by the legacy of the different cover crops ($F_{7,28} = 9.87$, $p < 0.0001$; Figure 3a). Barley grown on fallow plots performed poorer compared to barley grown on plots with a cover crop legacy, yet also the type of cover crop grown affected the barley biomass. The legacy of the vetch-radish cover crop mixture resulted in the highest barley biomass, especially when compared with fallow, oat, and vetch legacies (Figure 3a). The barley grain yield was also significantly affected by the cover crops ($F_{7,28} = 3.57$, $p < 0.01$; Figure 3c). The cover crop mixture legacies of vetch-radish and oat-radish resulted in the highest barley grain yield (5.6 and 5.4 t/ha, respectively), whereas grain yield was lowest for barley grown on fallow soil (4.4 t/ha). Other barley traits showed a similar pattern, and barley grown on fallow soil always underperformed. Barley N uptake was strongly affected by the cover crop legacies ($F_{7,28} = 14.12$, $p < 0.0001$; Figure 3b). A rough estimate is difficult only from the in-situ measurements as we lack root measurements this year to estimate the total from cover crops. The total N in the aboveground barley biomass was about 90 kg/ha for barley grown after fallow and up to 150 kg N/ha for barley after the cover crop vetch-radish (Figure 3b). This indicates that all nitrogen above 90 kg N/ha (i.e. up to 60 kg N/ha) is coming from N mineralised from the cover crops as the N in the barley grown after fallow originates from the mineral N fertiliser applied plus the N mineralised from the inherent SOM. N uptake was highest in barley grown after the cover crop mixtures vetch-radish or oat-radish and was lowest in barley grown after oat or in fallow soil (Figure 3b). Barley grain N concentration was significant different between barley grown in soil with a cover crop legacy versus on fallow soil ($F_{7,28} = 6.18$, $p < 0.0001$; Figure 3d).

3.2 | Remote sensing analysis during crop development

The temporal pattern in barley CNC was significantly affected by the cover crop legacies (Figure 4). Barley grown on plots with a legacy of the cover crop mixtures vetch-radish or oat-radish showed significantly higher

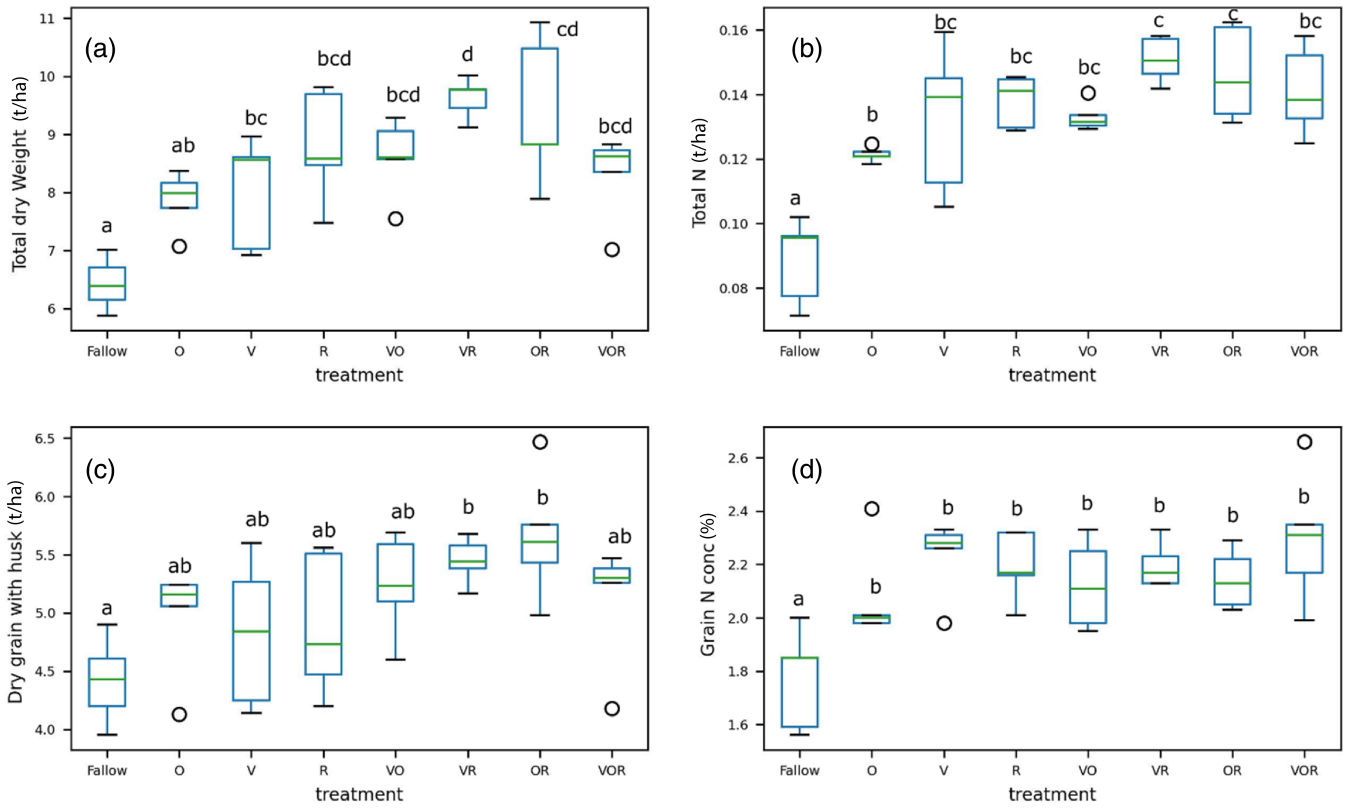

FIGURE 3 Barley characteristics at harvest in response to the cover crop legacies: barley (a) biomass (t dw/ha), (b) nitrogen content (t/ha), (c) grain yield (t dw/ha), and (d) grain N content (%). O, oats; R, radish; V, vetch and their combinations, and fallow. Data are shown as boxplots, $n = 5$, significance level α=0.05.

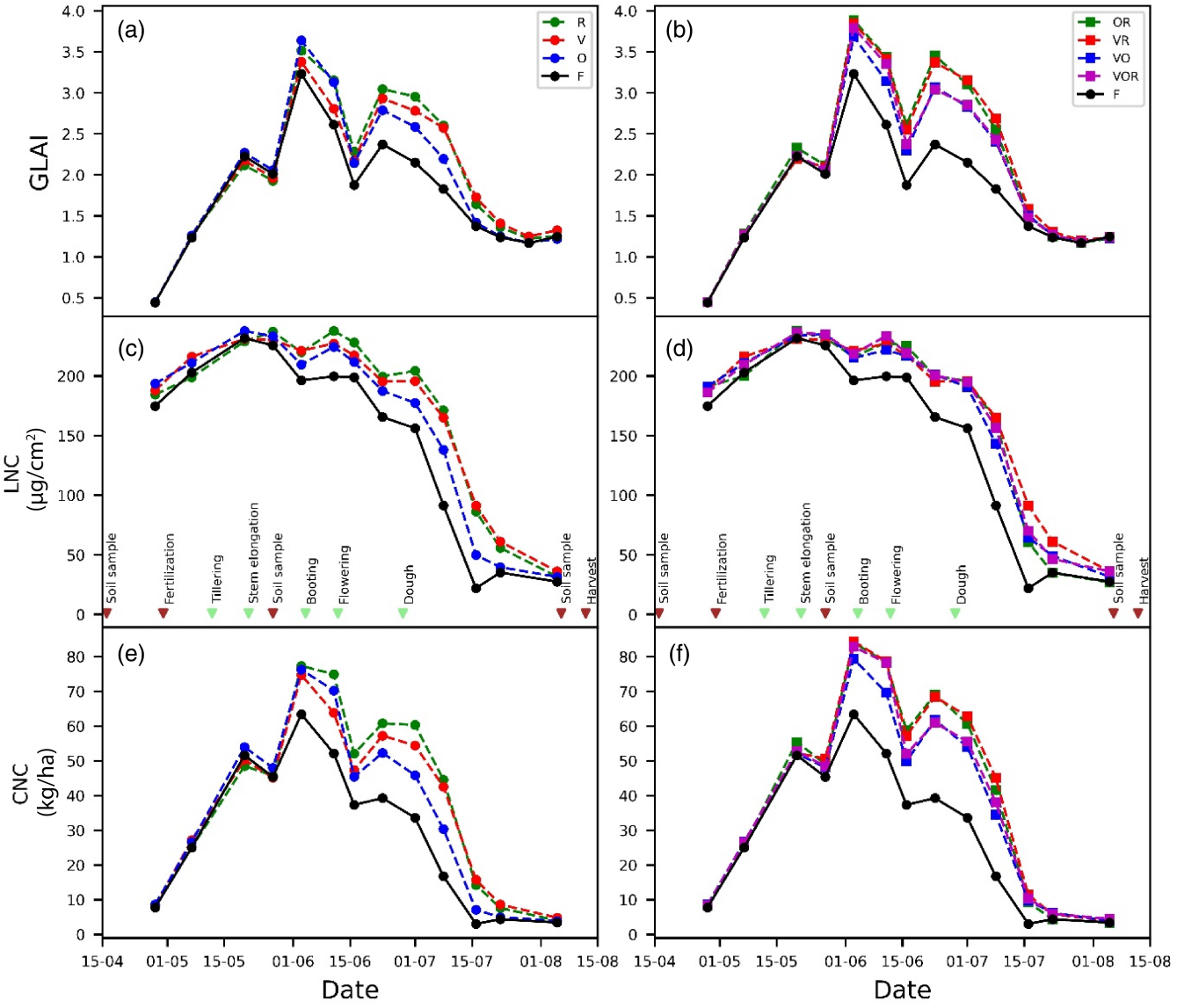

FIGURE 4 Temporal dynamics of remote sensing variables (season 2021) of green leaf area index (GLAI), leaf nitrogen content (LNC), and canopy N content (CNC) for barley response to the legacy of the cover crop monocultures (O, oats; R, radish; V, vetch) and the fallow (F) (panels a, c, e), and the cover crop mixtures (panels b, d, f). For comparison, barley response to fallow (black) is shown in all figure panels. Green coloured arrows indicate barley developmental stages; brown arrows indicate time of fertilisation, harvest date, and soil sample dates.

CNC levels compared to barley grown on fallow soil ($p < 0.05$; Figure 4f). For the monoculture cover crop legacies, radish promoted the barley CNC levels most, with marginally significantly higher values compared to barley grown on fallow soil ($p = 0.056$).

The increase in barley CNC over time was most notable from the stage of barley tillering until flowering (Figure 4). The period during which barley CNC increased was notably shorter in barley growing on fallow soil where already at start of stem elongation the barley CNC started to level off (Figure 4e,f). In plots with a legacy of radish, either as monocrop or in a mixture, barley CNC increased to the highest level observed, and this was achieved by the start of flowering (Figure 4e,f).

The comparison of the critical barley developmental stages such as stem elongation, booting, flowering, and dough development displayed differences in CNC levels among the cover crop treatments. Except for the tillering period when there were no significant differences, barley grown after fallow underperformed across the development stages (Figure S2). During booting stage, barley grown after vetch-radish or after oat-radish showed better performances compared to barley grown after fallow or vetch. This trend continued towards the flowering date when barley grown after cover crop mixtures started to show a significant difference in CNC level ($p < 0.05$). Later, during the senescence period, the pattern of barley CNC was in line with the total N values measured at harvest (Figure 3b).

Comparing maps of barley crop canopy traits at crucial crop development stages can help to identify the effects of soil variation across the field due to cover crop legacies and other potential sources of variation. Field maps of the barley CNC across the 40 plots on successive dates representing the booting, milk, and dough development stage of barley show the spatial and temporal variation of the barley canopy N (Figure 5). Across all developmental stages, barley grown on fallow plots showed relatively low values of N compared to the barley plants grown in plots with a cover crop legacy (Figure 5). Barley grown in block 5 (plots 33–40) displayed higher values than barley grown in the other blocks (see also Figure S2). The lowest range of CNC values was found around the barley milk stage of barley which was associated with low soil water availability during this period (Figure 6c,d).

3.3 | Relationship between crop N-uptake dynamics and soil properties

The soil microbial biomass and composition in terms of saprotrophic bacteria and fungi at the start of the main crop growing season mid-April was not significantly affected by the legacy effects of the cover crop treatments (Table S4). The soil microbial F:B ratio and GP:GN were also not significantly different among the cover crop legacies (Table S4). The period will visualise any differences in the microbial communities after the use of the different cover crop treatments for several years. The timing was also decided after the cover crop incorporation and cash crop seeding to check the composition and microbial biomass at the start of the cover crop decomposition.

Soil mineral N levels were significantly affected by the different cover crop legacies early in the barley growing season, but this effect faded over time (Figure S3). On 16 April, plots with a cover crop legacy of vetch showed significantly higher levels of soil mineral N compared to plots with a fallow legacy. Two weeks later, on 30th April, mineral fertiliser at a dose of 81 kg N per ha was applied to all the plots. However, a month later, on 27 May, the level of mineral N in soil was only 10 kg N per ha on average across all cover crop legacies. Close to the barley harvest date, on 6 August, the soil mineral N levels were below 10 kg N per ha.

The low levels of soil mineral N in all plots at the end of May, despite the addition of mineral fertiliser at the end of April, indicate high N uptake by barley during May which coincided with the increase in barley CNC (Figure 5). In the in-situ soil cores where we

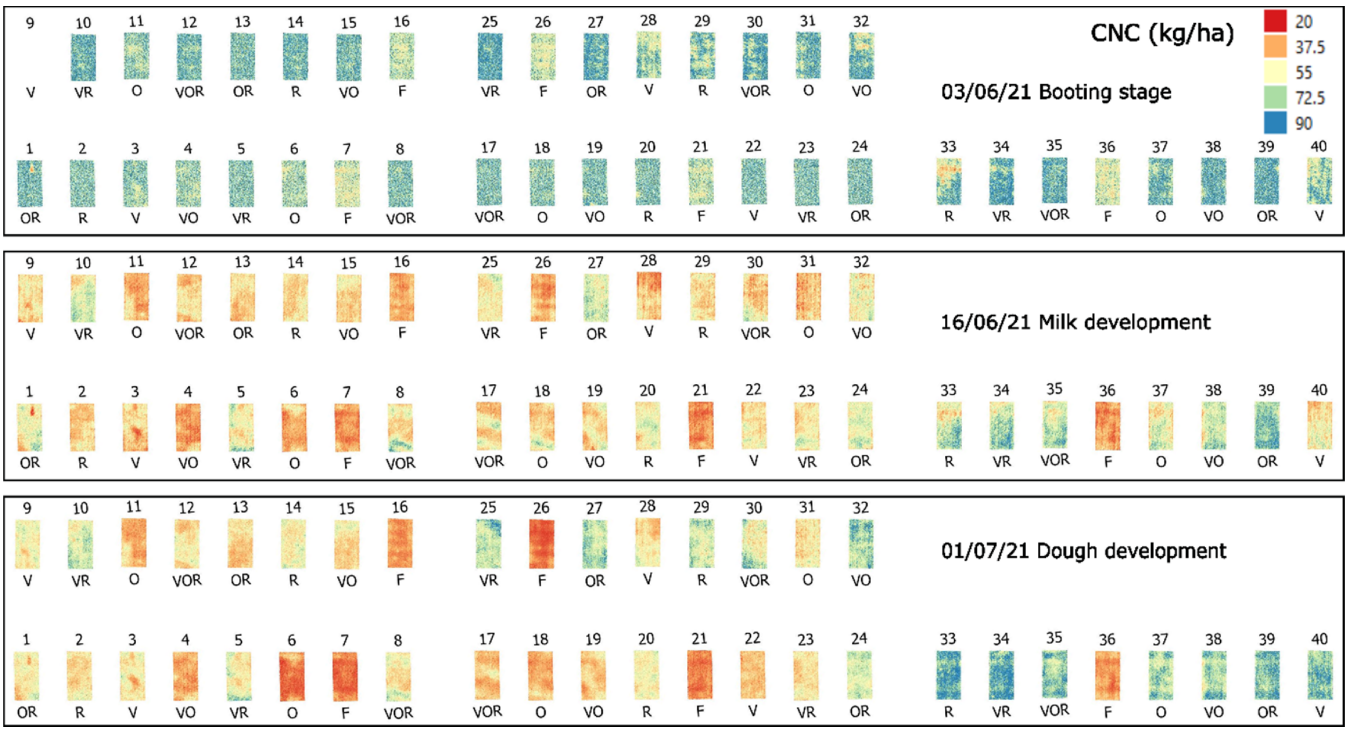

FIGURE 5 Spatial representation of barley canopy N content (CNC) (kg/ha) across the 40 plots in the field experiment on three dates at different development stages of barley. Rectangles represent the plots, and letters under the rectangles indicate the cover crop treatment that preceded the barley growth.

excluded barley roots from 27th May till harvest in August, we found no significant difference among the cover crop legacy treatments. Similarly, the amount of mineral N trapped by the resin bags located at the bottom of the in-situ soil cores showed no significant difference (Figure S4). The combination of the two results indicates that we likely missed a pool of N available for the plants but not quantified by the root-excluded in-situ coring + resin bag technique, such as N_2, which was likely lost through denitrification.

Comparing the temporal patterns of barley CNC, soil moisture and soil mineral N availability shows that despite the different mineral N levels at the beginning of the growing season, the available N dropped below 20 kg/ha before the water stress period (Figure 6). In terms of soil water content (SWC), we notice a clear response with the rainfall events and no difference in the patterns among the cover crop treatments. Table S5 displays the max, min and range of each SWC timeseries per treatment.

4 | DISCUSSION

We aimed to test the potential of UAV-based imaging for the characterisation of the temporal dynamics of main crop development in response to soil health legacy effects of cover crop monocultures and mixtures. Despite only having 1 year of UAV data season of a medium-term cover crop experiment for the specific crop in the rotation, we found that cover crop legacies promoted the development of the main crop in terms of final above-ground biomass, grain yield, N-uptake, and grain quality (grain N concentration). This work lays the foundation for future research across multiple crops and field sites and the importance of moving to long-term cover crop experiments. Several studies displayed similar effects of cover crops on main crops (Barel et al., 2018; Elhakeem et al., 2021; Finney et al., 2016). However, the choice of which cover crop to grow also matters as we found the highest average grain yield and N-uptake in barley grown after cover crop mixtures vetch-radish and oat-radish. These results are in line with the finding that cover crops with radish can promote N retention in the system across seasons (Elhakeem et al., 2023). Furthermore, we showed using UAV remote sensed data that the temporal dynamics of the barley CNC differ between cover crop legacies, notably between fallow, oat and vetch-radish, and oat-radish mixtures.

The different soil N supply rates to the plant can make an essential contribution to the final crop performance by releasing the N at the time the crop is able to take it up, thus reducing N losses compared to using only inorganic fertilisers (Abdalla et al., 2019; Barel et al., 2018). Mineral N for barley was provided by mineral fertiliser and N mineralisation from fresh and old organic matter by the

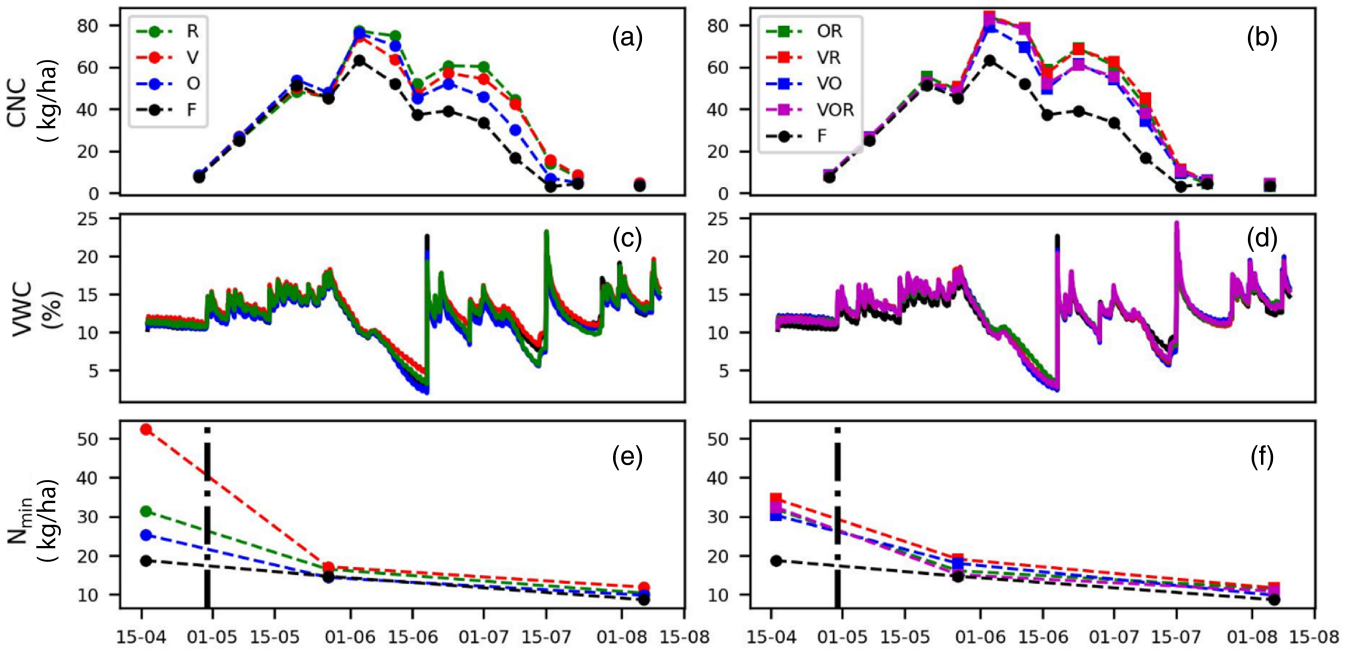

FIGURE 6 Temporal dynamics of barley canopy nitrogen content (CNC; upper row), soil moisture content (VWC; middle row), and mineral N (N_{min}; lower row) for the eight different cover crop treatments. The fallow (F) treatment (black) is repeated in the two columns for comparison. O, oats; R, radish; V, vetch and their combinations. The vertical black line displays the fertilisation date. For sake of clarity, the graphs divided into a + b and c + d and e + f.

soil biota. Given the low levels of soil mineral N at the end of May, N mineralisation was essential for crop N provisioning during the rest of the barley growing season. The temporal curves of barley CNC show lower values for barley growing on fallow soil. Barley CNC was second lowest when grown on oat legacy plots, which was expected due to the relatively high C:N ratio and lignin concentration of grass cover crops (Barel et al., 2019; Jahanzad et al., 2016). The higher N release and subsequent N uptake by barley, as reflected in the barley canopy N levels in barley grown after radish and mixtures with radish, can be explained by the combination of relatively high cover crop biomass and low lignin content and moderate C:N, compared to the legacy of vetch (relatively low C:N ratio but high lignin content and low biomass) and oat (high C:N ratio but high biomass). Both fallow and oat legacy supplied less N to barley than the other cover crop legacies, which is reflected in the temporal pattern of barley CNC as monitored using the drone-derived data. The remote sensing information complements the in-situ data as the low soil mineral N levels in May and August indicate that barley took up nearly all available N, and that the barley N uptake was to a large extent enabled by N mineralisation from the organic matter (including cover crop residues) in the soil. The rapid decline of soil mineral N despite the addition of mineral N fertiliser during the barley early development phase (April–May) can be attributed to both barley N uptake and N losses through leaching and gaseous emission.

The ability of UAV-based remote sensing to calculate GLAI and crop N uptake at high resolution in space and time enables high-resolution mapping of crop performance to examine field heterogeneity and assist in monitoring and managing the temporal dynamics of the soil legacies of cover crops. Using in-situ SPAD data to calculate the crop characteristics together with the GLAI derived by UAV imagery (Nguy-Robertson et al., 2014) enabled us to reconstruct the N dynamics of barley throughout its growing season. The multi-spectral camera used in this research also includes, next to spectral bands in visible and NIR, a band in the red-edge part of the spectrum. Using the Micasense multispectral camera, we followed the general protocol for acquisition of multispectral UAV images. We applied radiometric calibration including the measurements of the reference panels during the image acquisition. For the geometrical correction, we included nine ground control points in the photogrammetric processing. The timing of the UAV flight was around noon under constant light and atmospheric conditions. In most cases, this was under open sky conditions, but on some dates, acquisition was done under complete but homogeneous cloud coverage.

The dynamics we observed revealed that barley N uptake mainly occurred between tillering and stem elongation in fallow plots yet continued till flowering in plots with a cover crop legacy, especially with cover crop mixtures containing radish. Beneficial effects of radish cover crops in N retention during their growth and its support of main crop productivity upon decomposition are in line with earlier findings (Barel et al., 2018; Elhakeem et al., 2023), but these studies could not capture the temporal dynamics during crop development. Damian et al. (2017) found the NDVI, calculated using a portable ground sensor and an UAV, effectively evaluated the variability in a black oats crop and the cycled nutrients. In terms of cover crop, the dry weight of black oats and the accumulated N and other nutrients significantly correlated with soybean grain yield, and the organic matter in the soil had the most influence on the yield (Damian et al., 2017). Yuan et al. (2021) also found that cover crops affected the main crop but significantly reduced early- to mid-season corn and soybean NDVI compared to non-cover crop treatments, and these differences diminished over the growing season. Despite the variability in measurements, yields were not different with cover crops in contrast to our results, possibly due to the relatively low cover crop biomass observed in their experiment (Yuan et al., 2021).

The temporal dynamics in barley N uptake due to cover crop legacies and weather conditions were also visible in the barley CNC spatial variation before and after the drought period. The values of barley CNC across the field show that in most plots, barley could bounce back from the low values mid-June during milk development, but that CNC of barley on fallow plots could not recover well, hinting at cover crop mediated improvement of soil health resilience (Blanco-Canqui & Ruis, 2020). It is worth mentioning that all the high levels of barley CNC during the dough stage (Figure S2) are from barley grown in field block 5 (Figure 5); in this block, SOM levels were also highest.

The GLAI dynamics displayed a drop on 16th of June which could be attributed to the dry period as evidenced by the soil moisture sensor data and resulting from the reduced rainfall in that period. In addition, SPAD cannot discriminate between light absorption or reflection and a decrease of transmittance, for example, due to low leaf water content that can result in high SPAD values and thereby be mistaken as chlorophyll increase (Martínez & Guiamet, 2004). To reduce such effects, there is potential for other VIs to be tested (Argento et al., 2022; Clevers & Kooistra, 2012; Söderström et al., 2017) or even a combination of indices that can include plant water stress (Yang et al., 2020). Future work can improve the

parameterisation between in-situ and UAV-derived data, by enhanced soil filtering and potentially by combining with a process-based model that can assist in identifying stress periods and modify the relationship between in-situ and remote sensed data.

The selection of soil PLFA analysis as method to characterise (biological) soil health is supported by the fact that this method enables a quantitative assessment of the functional composition of the saprotrophic soil microbial community and has been widely used in soil health assessment (Norris et al., 2020). PLFAs enable, with the same extraction method, the quantification of saprotrophic bacterial and fungal biomass, F:B ratio, and GP and GN bacteria, unlike other methods available to date (Fierer et al., 2021). Furthermore, quantitative data of soil bacterial and fungal biomass can assist in soil carbon and nitrogen model simulations. We acknowledge that PLFA analysis has its limitations and that DNA- and RNA-based approaches and enzyme assays can provide further insights into the taxonomic composition of the soil microbial communities and their functional attributes, for example, soil borne pathogens and nitrifier abundances; however, these abundances may not necessarily correlate with their actual levels of activity, as shown for nitrification rates (Fierer et al., 2021). For our study, we did not require the level of detail from DNA-based techniques as our study focussed on the different temporal dynamics of the barley CNC that reflect the different soil health effects of the cover crop treatments through their impact on nutrient mineralisation by the soil biota. At the start of the barley growing season and 2 weeks after the incorporation of the cover crops into the soil, neither the microbial biomass nor the community composition differed significantly between the cover crop legacies. Therefore, differential impacts on N mineralisation are likely due to differences in microbial activity and efficiency in decomposing the cover crop material. In line with our findings, earlier work demonstrated enhanced microbial decomposition activity in sandy soil with a legacy of radish cover crops, which was attributed to the high decomposability and quantity of the radish plant material with low lignin and low C:N ratio (Barel et al., 2019). Our microbial biomass data of the soil bacteria are lower compared to the values of Barel et al. (2019), which may be due to lower organic matter input or colder spring in our experiment. Across our cover crop treatments, soil temperature and moisture did not differ significantly. In a meta-analysis of earlier studies on cover crops and their impact on soil microbial biomass, it was found that generally cover crops increase soil microbial biomass (Muhammad et al., 2021). However, as the authors discussed, the impact of the cover crops varied widely and were dependent on the soil and climatic conditions, with more notable increases in microbial biomass in soils with pH above 6 and in clay/clay-loam soils than in sandy soils.

The integration of the different soil physical, chemical, and biological indicators to describe soil health and soil functions can better inform farmers by providing a more comprehensive approach (Norris et al., 2020). As discussed above, we found that our cover crop treatments significantly affect soil biological health parameters, notably the provisioning of soil mineral N through the decomposition of the cover crop residues via soil microbial activity, and not via differences in soil microbial biomass at the start of the main crop growing season. With respect to soil physical and chemical soil health parameters, earlier research on cover crops demonstrated a reduction in bulk density, and increase in hydraulic conductivity, porosity, and water infiltration and retention (Gabriel et al., 2019; Haruna et al., 2020) and in SOM (Ding et al., 2006) in soil with versus without cover crops. However, in our experiment, we did not see a difference in water availability in the soil in relation to the different cover crop treatments. This can be attributed to the fact that average levels of SOM did not differ between the cover crop treatments and were more affected by the spatial location in the field (differences between field blocks). Furthermore, our data were collected in the fifth year of the experiment and it is known that changes in SOM and soil hydrological properties in response to cover crops can take a longer time before they become apparent, and may show up stronger in a no-till compared to a tilled system (Gabriel et al., 2019; Villamil et al., 2006).

The results of our experiment give researchers and stakeholders more insights into the contribution of the distinct types of cover crops on the N dynamics in the cropping system. Moreover, this research investigates the suitability of a remote sensing-based approach for measuring the components of the N balance (Kanning et al., 2018). Furthermore, our work illustrates the potential of remote sensing to monitor the dynamics of crop N uptake under different cover crop legacies, which enables the reduction of destructive fieldwork while providing higher spatial and temporal resolution. Follow-up work of data assimilation and mechanistic models will assist in simulating and predicting the temporal changes in the soil, cover crop, and main crop development throughout the seasons (Jin et al., 2018; Vereecken et al., 2016). Especially, the connection with remote sensing and the ability to have a high temporal resolution of observations through drones can improve the model performance. That approach can also help to optimise fertilisation timing for better crop N uptake by quantifying the N levels spatially and temporally across multiple fields. The main goal of this approach is to improve the monitoring and soil health-based management of N cycling in

agricultural fields and better represent the underlying mechanisms.

5 | CONCLUSION

Cover crop legacies generate distinct temporal dynamics in N availability and main crop N uptake which can be adequately monitored using UAV-based remote sensing of crop CNC. In particular, the legacy of cover crop mixtures containing radish (specifically vetch-radish and oat-radish) enhanced growth and N uptake in barley. This led to an increased yield of superior quality grain.

The VI derived from UAV (Cl_{red}) facilitates the upscaling of vegetation parameters at the plot to field level over time. UAV data collection allows for the quantification of spatial variability and the temporal evolution of crop N absorption throughout the growing season. This data can be utilised for upscaling, model data assimilation schemes, and the development of precision field management tools.

In our field experiment, we did not see significant differences between the fallow and the different cover crop treatments with respect to the soil physical parameters and the soil biological parameter soil microbial biomass at the start of the main crop season. However, we did see significant differences with the main crop N uptake over the growing season, which is due to differences in the dynamics of N availability in the soil due to soil microbial activity.

AUTHOR CONTRIBUTIONS

Nikolaos-Christos Vavlas: Conceptualization (equal); data curation (lead); formal analysis (lead); methodology (equal); software (lead); visualization (lead); writing – original draft (lead). **Thijs Seubring:** Data curation (supporting); formal analysis (supporting); investigation (supporting); software (supporting); writing – review and editing (supporting). **Ali Elhakeem:** Conceptualization (supporting); data curation (lead); investigation (supporting); writing – review and editing (supporting). **Lammert Kooistra:** Conceptualization (equal); supervision (equal); writing – review and editing (equal). **Gerlinde B. De Deyn:** Conceptualization (equal); funding acquisition (lead); project administration (lead); supervision (equal); writing – review and editing (lead).

ACKNOWLEDGEMENTS

We would like to thank Claudio Screpanti for his careful review of the manuscript and valuable suggestions, Henk Martens for the assistance on PLFA analysis, and Peter van der Zee and Berry Onderstal for the UAV data acquisition. The project was supported with funding from the Syngenta (project: Soil health and the potential of remote sensing).

CONFLICT OF INTEREST STATEMENT

The authors declare no conflicts of interest.

DATA AVAILABILITY STATEMENT

The data that support the findings of this study will be openly available in Zenodo at https://doi.org/10.5281/zenodo.11190677 and on request from the authors.

ORCID

Nikolaos-Christos Vavlas https://orcid.org/0000-0003-0247-6064

REFERENCES

Abdalla, M., Hastings, A., Cheng, K., Yue, Q., Chadwick, D., Espenberg, M., Truu, J., Rees, R. M., & Smith, P. (2019). A critical review of the impacts of cover crops on nitrogen leaching, net greenhouse gas balance and crop productivity. *Global Change Biology*, *25*, 2530–2543. https://doi.org/10.1111/gcb.14644

Abdulraheem, M. I., Zhang, W., Li, S., Moshayedi, A. J., Farooque, A. A., & Hu, J. (2023). Advancement of remote sensing for soil measurements and applications: A comprehensive review. *Sustainability*, *15*, 15444. https://www.mdpi.com/2071-1050/15/21/15444/htm

Argento, F., Liebisch, F., Simmler, M., Ringger, C., Hatt, M., Walter, A., & Anken, T. (2022). Linking soil N dynamics and plant N uptake by means of sensor support. *European Journal of Agronomy*, *134*, 126462.

Bardgett, R. D., Hobbs, P. J., & Frostegard, A. (1996). Changes in soil fungal:bacterial biomass ratios following reductions in the intensity of management of an upland grassland. *Biology and Fertility of Soils*, *22*, 261–264.

Barel, J. M., Kuyper, T. W., de Boer, W., Douma, J. C., & De Deyn, G. B. (2018). Legacy effects of diversity in space and time driven by winter cover crop biomass and nitrogen concentration (L Cheng, Ed.). *Journal of Applied Ecology*, *55*, 299–310. https://doi.org/10.1111/1365-2664.12929

Barel, J. M., Kuyper, T. W., Paul, J., de Boer, W., Cornelissen, J. H. C., & De Deyn, G. B. (2019). Winter cover crop legacy effects on litter decomposition act through litter quality and microbial community changes (L Cheng, Ed.). *Journal of Applied Ecology*, *56*, 132–143. https://doi.org/10.1111/1365-2664.13261

Barry, K. E., Mommer, L., van Ruijven, J., Wirth, C., Wright, A. J., Bai, Y., Connolly, J., De Deyn, G. B., de Kroon, H., Isbell, F., Milcu, A., Roscher, C., Scherer-Lorenzen, M., Schmid, B., & Weigelt, A. (2019). The future of complementarity: Disentangling causes from consequences. *Trends in Ecology & Evolution*, *34*, 167–180.

Berger, K., Verrelst, J., Féret, J. B., Wang, Z., Wocher, M., Strathmann, M., Danner, M., Mauser, W., & Hank, T. (2020). Crop nitrogen monitoring: Recent progress and principal developments in the context of imaging spectroscopy missions. *Remote Sensing of Environment*, *242*, 111758.

Blanco-Canqui, H., & Ruis, S. J. (2020). Cover crop impacts on soil physical properties: A review. *Soil Science Society of America Journal*, *84*, 1527–1576. https://doi.org/10.1002/saj2.20129

Bligh, E. G., & Dyer, W. J. (1959). A rapid method of total lipid extraction and purification. *Canadian Journal of Biochemistry and Physiology*, *37*, 911–917. https://doi.org/10.1139/o59-099

Boegh, E., Houborg, R., Bienkowski, J., Braban, C. F., Dalgaard, T., Van Dijk, N., Dragosits, U., Holmes, E., Magliulo, V., Schelde, K., Di Tommasi, P., Vitale, L., Theobald, M. R., Cellier, P., & Sutton, M. A. (2013). Remote sensing of LAI, chlorophyll and leaf nitrogen pools of crop- and grasslands in five European landscapes. *Biogeosciences*, *10*, 6279–6307.

Bünemann, E. K., Bongiorno, G., Bai, Z., Creamer, R. E., De Deyn, G., de Goede, R., Fleskens, L., Geissen, V., Kuyper, T. W., Mäder, P., Pulleman, M., Sukkel, W., van Groenigen, J. W., & Brussaard, L. (2018). Soil quality—A critical review. *Soil Biology and Biochemistry*, *120*, 105–125. https://doi.org/10.1016/j.soilbio.2018.01.030

Clevers, J., Kooistra, L., & van den Brande, M. (2017). Using Sentinel-2 data for retrieving LAI and leaf and canopy chlorophyll content of a potato crop. *Remote Sensing*, *9*, 405. http://www.mdpi.com/2072-4292/9/5/405

Clevers, J. G. P. W., & Kooistra, L. (2012). Using hyperspectral remote sensing data for retrieving canopy chlorophyll and nitrogen content. *IEEE Journal of Selected Topics in Applied Earth Observations and Remote Sensing*, *5*, 574–583. https://ieeexplore.ieee.org/document/6096423/

Cortois, R., Schröder-Georgi, T., Weigelt, A., van der Putten, W. H., & De Deyn, G. B. (2016). Plant–soil feedbacks: Role of plant functional group and plant traits. *Journal of Ecology*, *104*, 1608–1617. https://doi.org/10.1111/1365-2745.12643

Cuaran, J., & Leon, J. (2021). Crop monitoring using unmanned aerial vehicles: A review. *Agricultural Reviews*, *42*, 121–132.

Damian, J. M., Santi, A. L., Fornari, M., Da Ros, C. O., & Eschner, V. L. (2017). Monitoring variability in cash-crop yield caused by previous cultivation of a cover crop under a no-tillage system. *Computers and Electronics in Agriculture*, *142*, 607–621.

Ding, G., Liu, X., Herbert, S., Novak, J., Amarasiriwardena, D., & Xing, B. (2006). Effect of cover crop management on soil organic matter. *Geoderma*, *130*, 229–239.

Dong, T., Meng, J., Shang, J., Liu, J., & Wu, B. (2015). Evaluation of chlorophyll-related vegetation indices using simulated Sentinel-2 data for estimation of crop fraction of absorbed photosynthetically active radiation. *IEEE Journal of Selected Topics in Applied Earth Observations and Remote Sensing*, *8*, 4049–4059. https://www.researchgate.net/publication/273059111_Evaluation_of_Chlorophyll-Related_Vegetation_Indices_Using_Simulated_Sentinel-2_Data_for_Estimation_of_Crop_Fraction_of_Absorbed_Photosynthetically_Active_Radiation

Elhakeem, A., Bastiaans, L., Houben, S., Couwenberg, T., Makowski, D., & van der Werf, W. (2021). Do cover crop mixtures give higher and more stable yields than pure stands? *Field Crops Research*, *270*, 108217.

Elhakeem, A., Porre, R. J., Hoffland, E., Van Dam, J. C., Drost, S. M., & De Deyn, G. B. (2023). Radish-based cover crop mixtures mitigate leaching and increase availability of nitrogen to the cash crop. *Field Crops Research*, *292*, 108803. https://linkinghub.elsevier.com/retrieve/pii/S0378429022003744

Erisman, J. W., Galloway, J. N., Seitzinger, S., Bleeker, A., Dise, N. B., Petrescu, A. M. R., Leach, A. M., & de Vries, W. (2013). Consequences of human modification of the global nitrogen cycle. *Philosophical Transactions of the Royal Society B: Biological Sciences*, *368*, 20130116.

Fierer, N., Wood, S. A., & Bueno de Mesquita, C. P. (2021). How microbes can, and cannot, be used to assess soil health. *Soil Biology and Biochemistry*, *153*, 108111. https://linkinghub.elsevier.com/retrieve/pii/S0038071720304077

Finney, D. M., White, C. M., & Kaye, J. P. (2016). Biomass production and carbon/nitrogen ratio influence ecosystem services from cover crop mixtures. *Agronomy Journal*, *108*, 39–52. https://doi.org/10.2134/agronj15.0182

Frostegard, A., & Baath, E. (1996). The use of phospholipid fatty acid analysis to estimate bacterial and fungal biomass in soil. *Biology and Fertility of Soils*, *22*, 59–65.

Frostegard, A., Tunlid, A., & Baath, E. (1993). Phospholipid fatty acid composition, biomass, and activity of microbial communities from two soil types experimentally exposed to different heavy metals. *Applied and Environmental Microbiology*, *59*, 3605–3617. https://doi.org/10.1128/aem.59.11.3605-3617.1993

Gabriel, J. L., Quemada, M., Martín-Lammerding, D., & Vanclooster, M. (2019). Assessing the cover crop effect on soil hydraulic properties by inverse modelling in a 10-year field trial. *Agricultural Water Management*, *222*, 62–71.

Godfray, H. C. J., Beddington, J. R., Crute, I. R., Haddad, L., Lawrence, D., Muir, J. F., Pretty, J., Robinson, S., Thomas, S. M., & Toulmin, C. (2010). Food security: The challenge of feeding 9 billion people. *Science*, *327*, 812–818.

Haruna, S. I., Anderson, S. H., Udawatta, R. P., Gantzer, C. J., Phillips, N. C., Cui, S., & Gao, Y. (2020). Improving soil physical properties through the use of cover crops: A review. *Agrosystems, Geosciences & Environment*, *3*, e20105. https://doi.org/10.1002/agg2.20105

Hedlund, K. (2002). Soil microbial community structure in relation to vegetation management on former agricultural land. *Soil Biology and Biochemistry*, *34*, 1299–1307. https://linkinghub.elsevier.com/retrieve/pii/S0038071702000731

Heijboer, A., ten Berge, H. F. M., de Ruiter, P. C., Jørgensen, H. B., Kowalchuk, G. A., & Bloem, J. (2016). Plant biomass, soil microbial community structure and nitrogen cycling under different organic amendment regimes; a 15N tracer-based approach. *Applied Soil Ecology*, *107*, 251–260.

Holland, J., Brown, J. L., MacKenzie, K., Neilson, R., Piras, S., & McKenzie, B. M. (2021). Over winter cover crops provide yield benefits for spring barley and maintain soil health in northern Europe. *European Journal of Agronomy*, *130*, 126363.

Hothorn, T., Bretz, F., & Westfall, P. (2008). Simultaneous inference in general parametric models. *Biometrical Journal*, *50*, 346–363. https://pubmed.ncbi.nlm.nih.gov/18481363/

Jago, R. A., Cutler, M. E. J., & Curran, P. J. (1999). Estimating canopy chlorophyll concentration from field and airborne spectra. *Remote Sensing of Environment*, *68*, 217–224.

Jahanzad, E., Barker, A. V., Hashemi, M., Eaton, T., Sadeghpour, A., & Weis, S. A. (2016). Nitrogen release dynamics and decomposition of buried and surface cover crop residues. *Agronomy Journal*, *108*, 1735–1741.

Jin, X., Kumar, L., Li, Z., Feng, H., Xu, X., Yang, G., & Wang, J. (2018). A review of data assimilation of remote sensing and

crop models. *European Journal of Agronomy*, *92*, 141–152. https://doi.org/10.1016/j.eja.2017.11.002

Kanning, M., Kühling, I., Trautz, D., & Jarmer, T. (2018). *Remote sensing high-resolution UAV-based hyperspectral imagery for LAI and chlorophyll estimations from wheat for yield prediction*. https://www.mdpi.com/journal/remotesensing

Kira, O., Nguy-Robertson, A. L., Arkebauer, T. J., Linker, R., & Gitelson, A. A. (2016). Informative spectral bands for remote green LAI estimation in C3 and C4 crops. *Agricultural and Forest Meteorology*, *218–219*, 243–249.

Lassaletta, L., Billen, G., Garnier, J., Bouwman, L., Velazquez, E., Mueller, N. D., & Gerber, J. S. (2016). Nitrogen use in the global food system: Past trends and future trajectories of agronomic performance, pollution, trade, and dietary demand. *Environmental Research Letters*, *11*, 095007.

Lenth, R., Singmann, H., Love, J., Buerkner, P., & Huerve, M. 2019. *Emmeans: Estimated marginal means, aka least-squares means*.

Levene, H. (1960). Robust tests for equality of variances. In I. Olkin (Ed.), *Contributions to probability and statistics* (pp. 278–292). Stanford University Press. https://cir.nii.ac.jp/crid/1573950400526848896

Lu, J., Cheng, D., Geng, C., Zhang, Z., Xiang, Y., & Hu, T. (2021). Combining plant height, canopy coverage and vegetation index from UAV-based RGB images to estimate leaf nitrogen concentration of summer maize. *Biosystems Engineering*, *202*, 42–54.

Mariotte, P., Mehrabi, Z., Bezemer, T. M., De Deyn, G. B., Kulmatiski, A., Drigo, B., Veen, G. F., van der Heijden, M. G. A., & Kardol, P. (2018). Plant–soil feedback: Bridging natural and agricultural sciences. *Trends in Ecology & Evolution*, *33*, 129–142.

Markwell, J., Osterman, J. C., & Mitchell, J. L. (1995). Calibration of the Minolta SPAD-502 leaf chlorophyll meter. *Photosynthesis Research*, *46*, 467–472.

Martínez, D. E., & Guiamet, J. J. (2004). Distortion of the SPAD 502 chlorophyll meter readings by changes in irradiance and leaf water status. *Agronomie*, *24*, 41–46.

Martínez-García, L. B., Korthals, G., Brussaard, L., Jørgensen, H. B., & De Deyn, G. B. (2018). Organic management and cover crop species steer soil microbial community structure and functionality along with soil organic matter properties. *Agriculture, Ecosystems and Environment*, *263*, 7–17.

Muhammad, I., Wang, J., Sainju, U. M., Zhang, S., Zhao, F., & Khan, A. (2021). Cover cropping enhances soil microbial biomass and affects microbial community structure: A meta-analysis. *Geoderma*, *381*, 114696.

Näsi, R., Viljanen, N., Kaivosoja, J., Alhonoja, K., Hakala, T., Markelin, L., & Honkavaara, E. (2018). Estimating biomass and nitrogen amount of barley and grass using UAV and aircraft based spectral and photogrammetric 3D features. *Remote Sensing*, *10*, 1082.

Nguy-Robertson, A. L., Peng, Y., Gitelson, A. A., Arkebauer, T. J., Pimstein, A., Herrmann, I., Karnieli, A., Rundquist, D. C., & Bonfil, D. J. (2014). Estimating green LAI in four crops: Potential of determining optimal spectral bands for a universal algorithm. *Agricultural and Forest Meteorology*, *192–193*, 140–148.

Norris, C. E., Bean, G. M., Cappellazzi, S. B., Cope, M., Greub, K. L. H., Liptzin, D., Rieke, E. L., Tracy, P. W., Morgan, C. L. S., & Honeycutt, C. W. (2020). Introducing the North American project to evaluate soil health measurements. *Agronomy Journal*, *112*, 3195–3215. https://doi.org/10.1002/agj2.20234

Nuijten, R. J. G., Kooistra, L., & De Deyn, G. B. (2019). Using unmanned aerial systems (UAS) and object-based image analysis (OBIA) for measuring plant-soil feedback effects on crop productivity. *Drones*, *3*, 1–14.

Ohyama, T. (2010). Nitrogen as a major essential element of plants. *Nitrogen Assimilation in Plants*, *37*, 1–17. https://www.researchgate.net/profile/Takuji-Ohyama/publication/234135771_Nitrogen_as_a_major_essential_element_of_plants/links/0c96051ac0b614543a000000/Nitrogen-as-a-major-essential-element-of-plants.pdf

Pinheiro, J., Bates, D., DebRoy, S., Sarkar, D., & R Core Team. (2019). *nlme: Linear and nonlinear mixed effects models* (pp. 1–140). https://svn.r-project.org/R-packages/trunk/nlme/

Ramírez-García, J., Carrillo, J. M., Ruiz, M., Alonso-Ayuso, M., & Quemada, M. (2015). Multicriteria decision analysis applied to cover crop species and cultivars selection. *Field Crops Research*, *175*, 106–115.

Risch, A. C., Zimmermann, S., Ochoa-Hueso, R., Schütz, M., Frey, B., Firn, J. L., Fay, P. A., Hagedorn, F., Borer, E. T., Seabloom, E. W., Harpole, W. S., Knops, J. M. H., McCulley, R. L., Broadbent, A. A. D., Stevens, C. J., Silveira, M. L., Adler, P. B., Báez, S., Biederman, L. A., … Moser, B. (2019). Soil net nitrogen mineralisation across global grasslands. *Nature Communications*, *10*, 4981.

Scavo, A., Fontanazza, S., Restuccia, A., Pesce, G. R., Abbate, C., & Mauromicale, G. (2022). The role of cover crops in improving soil fertility and plant nutritional status in temperate climates. A review. *Agronomy for Sustainable Development*, *42*, 93.

Shapiro, S. S., & Wilk, M. B. (1965). An analysis of variance test for normality (complete samples). *Biometrika*, *52*, 591–611. https://doi.org/10.1093/biomet/52.3-4.591

Söderström, M., Piikki, K., Stenberg, M., Stadig, H., & Martinsson, J. (2017). Producing nitrogen (N) uptake maps in winter wheat by combining proximal crop measurements with Sentinel-2 and DMC satellite images in a decision support system for farmers. *Acta Agriculturae Scandinavica, Section B—Soil & Plant Science*, *67*, 637–650. https://doi.org/10.1080/09064710.2017.1324044

Takoutsing, B., Weber, J., Aynekulu, E., Rodríguez Martín, J. A., Shepherd, K., Sila, A., Tchoundjeu, Z., & Diby, L. (2016). Assessment of soil health indicators for sustainable production of maize in smallholder farming systems in the highlands of Cameroon. *Geoderma*, *276*, 64–73.

Thorup-Kristensen, K., Magid, J., & Jensen, L. S. (2003). Catch crops and green manures as biological tools in nitrogen management in temperate zones. *Advances in Agronomy*, *79*, 227–302. https://www.researchgate.net/publication/223784980_Catch_crops_and_green_manures_as_biological_tools_in_nitrogen_management_in_temperate_zones

van der Meij, B., Kooistra, L., Suomalainen, J., Barel, J. M., & de Deyn, G. B. (2017). Remote sensing of plant trait responses to field-based plant-soil feedback using UAV-based optical sensors. *Biogeosciences*, *14*, 733–749.

Vavlas, N.-C., Waine, T. W., Meersmans, J., Burgess, P. J., Fontanelli, G., & Richter, G. M. (2020). Deriving wheat crop productivity indicators using Sentinel-1 time series. *Remote Sensing*, *12*, 2385. https://www.mdpi.com/2072-4292/12/15/2385

Vereecken, H., Schnepf, A., Hopmans, J. W., Javaux, M., Or, D., Roose, T., & Vanderborght, J. (2016). Modelling soil processes: Review, Key challenges and new perspectives. *Vadose Zone Journal*, *15*, 1–57. https://cpb-us-e2.wpmucdn.com/faculty.sites.uci.edu/dist/f/94/files/2016/04/111.pdf

Villamil, M. B., Bollero, G. A., Darmody, R. G., Simmons, F. W., & Bullock, D. G. (2006). No-till corn/soybean systems including winter cover crops. *Soil Science Society of America Journal*, *70*, 1936–1944. https://doi.org/10.2136/sssaj2005.0350

Vos, J., & Bom, M. (1993). Hand-held chlorophyll meter: A promising tool to assess the nitrogen status of potato foliage. *Potato Research*, *36*, 301–308.

Wild, J., Kopecký, M., Macek, M., Šanda, M., Jankovec, J., & Haase, T. (2019). Climate at ecologically relevant scales: A new temperature and soil moisture logger for long-term microclimate measurement. *Agricultural and Forest Meteorology*, *268*, 40–47. https://linkinghub.elsevier.com/retrieve/pii/S0168192318304118

Xie, Q., Dash, J., Huang, W., Peng, D., Qin, Q., Mortimer, H., Casa, R., Pignatti, S., Laneve, G., Pascucci, S., Dong, Y., & Ye, H. (2018). Vegetation indices combining the red and red-edge spectral information for leaf area index retrieval. *IEEE Journal of Selected Topics in Applied Earth Observations and Remote Sensing*, *11*, 1482–1492.

Yang, M., Hassan, M. A., Xu, K., Zheng, C., Rasheed, A., Zhang, Y., Jin, X., Xia, X., Xiao, Y., & He, Z. (2020). Assessment of water and nitrogen use efficiencies through UAV-based multispectral phenotyping in Winter wheat. *Frontiers in Plant Science*, *11*, 927.

Yuan, M., Burjel, J. C., Martin, N. F., Isermann, J., Goeser, N., & Pittelkow, C. M. (2021). Advancing on-farm research with UAVs: Cover crop effects on crop growth and yield. *Agronomy Journal*, *113*, 1071–1083.

Zelles, L. (1999). Fatty acid patterns of phospholipids and lipopolysaccharides in the characterisation of microbial communities in soil: A review. *Biology and Fertility of Soils*, *29*, 111–129.

Zelles, L., Bai, Q. Y., Ma, R. X., Rackwitz, R., Winter, K., & Beese, F. (1994). Microbial biomass, metabolic activity and nutritional status determined from fatty acid patterns and poly-hydroxybutyrate in agriculturally-managed soils. *Soil Biology and Biochemistry*, *26*, 439–446. https://linkinghub.elsevier.com/retrieve/pii/0038071794901759

Zhang, J., Hu, Y., Li, F., Fue, K. G., & Yu, K. (2024). Meta-analysis assessing potential of drone remote sensing in estimating plant traits related to nitrogen use efficiency. *Remote Sensing*, *16*, 838.

SUPPORTING INFORMATION

Additional supporting information can be found online in the Supporting Information section at the end of this article.

How to cite this article: Vavlas, N.-C., Seubring, T., Elhakeem, A., Kooistra, L., & De Deyn, G. B. (2024). Remote sensing of cover crop legacies on main crop N-uptake dynamics. *European Journal of Soil Science*, *75*(5), e13582. https://doi.org/10.1111/ejss.13582